



Research Paper

Land cover change detection using GIS and remote sensing techniques: A spatio-temporal study on Tanguar Haor, Sunamganj, Bangladesh



Md. Inzamul Haque*, Rony Basak

Department of Geography and Environment, Shahjalal University of Science & Technology, Sylhet 3114, Bangladesh

ARTICLE INFO

Article history:

Received 28 March 2016

Revised 15 December 2016

Accepted 20 December 2016

Available online 3 January 2017

Keywords:

Tanguar Haor

Wetland

Landsat

Land cover change

ABSTRACT

Tanguar Haor is one of the two listed Ramsar Site of this country which contains a rich amount of biodiversity as well as a highly productive ecosystem. But the valuable landscape undergoes a radical change in its form over the decades. This study uses past and recent satellite data to evaluate the typical landscape change over the decades. Both pre-classification and post classification change detection approach was used to assess the change result from 1980 to 2010. In pre-classification approach CVA, NDVI and NDWI analysis were implemented to assess the change scenario. Maximum likelihood supervised classification technique was performed to create the signature class of significant land cover category (deep water, shallow water, vegetation, and settlement). After ensuring satisfactory accuracy value for each classified image a detail post classification change detection analysis was executed. Image differencing, statistical change detection techniques (transition probability matrix), change dynamics analysis was also operated to evaluate the statistics of past change relative to present. This study illustrated that, about 40% land cover of the total study area has been converted over 30 years period. Forested and high land vegetation's are disappearing rapidly, deep water bodies consist of large lakes are becoming the rare feature of the study area. Widespread development of settlement and dominant shallow water feature are converting the natural wetland a permanent low lying agricultural land.

© 2016 National Authority for Remote Sensing and Space Sciences. Production and hosting by Elsevier B.V. This is an open access article under the CC BY-NC-ND license (<http://creativecommons.org/licenses/by-nc-nd/4.0/>).

1. Introduction

1.1. Background

Wetlands include world heritage sites with significant values to ecological, biologic, zoological, limnological, or hydrological settings, including such phenomena as thermal features and underground rivers (Blasco and Aizpuru, 1997). Tanguar Haor is one of the largest wetland systems in the northeast region of Bangladesh. It is also said to be a part of world's largest geosynclines (Sobhan et al., 2012). Tanguar Haor plays a vital part in the economy of Bangladesh with its natural richness and diversity. Both human-induced and natural land cover changes can influence the global change because of its interaction with terrestrial ecosystem (Houghton, 1994), biodiversity and landscape ecology (Reid et al., 2000). In addition, it reflects the human impacts on environment

at various temporal and spatial scales (Lopez et al., 2006). Therefore, accurate and up-to-date land use/cover information is essential for environmental planning, to understand the impact on terrestrial ecosystem (Muttilanon and Tripathi, 2005) and to achieve sustainable development (Alphan, 2003). Remote sensing (RS) and geographic information system (GIS) are now providing effective tools for advanced ecosystem and socio economic management. The collection of remotely sensed data facilitates the synoptic analyses of Earth – system function, patterning, and change at local, regional, and global scales over time; such data also provide an important link between intensive, localized ecological research and regional, national and international conservation and management of biological diversity (Wilkie and Finn, 1996).

1.2. Statement of the problem

As every living being is dependent on the natural land cover, temporal land cover change in land cover can reshape the whole scenario of an ecosystem. Tanguar Haor is facing overwhelming threats due to natural resource depletion, soil erosion, forest degradation, habitat degradation, water imbalance, unbalanced human interference and illegal poaching (Sobhan et al., 2012).

Peer review under responsibility of National Authority for Remote Sensing and Space Sciences.

* Corresponding author.

E-mail addresses: sazal.edu@outlook.com, sazal.geesust@gmail.com (M.I. Haque), rbasak-gee@sust.edu (R. Basak).

According to Information Sheet on Ramsar Site (RIS) – Swamp forests that were once common at the haor, have now become very rare due to clearing, cutting and burning, and the last vestiges remain at Rangchi, in the southwestern part of the haor. This part consists of about 800 more than 100-year-old, pollarded *Barringtonia acutangula* (hijal) and *Pongamia pinnata* (koroch) trees. Reed beds dominated by *Phragmites karka* have been severely reduced in area because of collecting for fuel and thatch, and the conversion of marginal wetlands for agriculture. Certain species of aquatic plant that used to be common in the area, have now disappeared or become very rare, probably due to a combination of over-utilization (of useful species) and changes in water quality (leading to poorer light penetration) (Mayor-gordove, 2014).

The current leasing system is seen as one of the major threats to sustainable management of the area, as it encourages maximum exploitation, and marginalizes the local community. Natural regeneration also become unknown in most of the places except in Foil-lar beel where there is some fleck remain (Sobhan et al., 2012).

Per BCAS (1997) surveys in their three sample mouza, forest areas have declined from 18% to 5% since 1971, and most of these areas have been convened into agricultural land.

Rapid population growth is a common and most serious factor around Bangladesh which also extremely influence this part of the country. During the last few decades, extensive agricultural activity has been expanded in the Haor area which force the Haor ecosystem to be a vast agricultural space. To cope up with population pressure more and more settlement is built around the Haor area which directly and indirectly disturb the wildlife specially the waterfowls and the fish habitats. Overwhelming use of agro-chemicals e.g. insecticides, fertilizers made the condition worst.

1.3. Objectives of the study

The main objective of the study was to evaluate the nature, significance, and rate of wetland change from 1980 to 2010. It also aimed to find out the areas of rapid change, magnitude of change and assess the past and present condition of Land Cover to understand the dynamics and trend of change.

1.4. Rationale of the study

Almost all the researchers defined Tanguar Haor as one of the most dynamic and productive natural wetland rests in Bangladesh. Tanguar Haor; listed in the Directory of Asian Wetlands (Scott, 1989) has been identified by NERP (1993a) as a key wetland site of international importance, especially because of its vital link in an international network of sites for migratory water birds.

Tanguar Haor comprises some dynamic functions responsible to behold the natural ecology of the region as well as the whole country include- groundwater recharge, groundwater discharge, flood control, shoreline stabilization, erosion control, sediment/toxicant retention, nutrient retention, biomass export, storm protection/windbreak, micro-climate stabilization, water transport, recreation/tourism (Ali, 2014).

Bangladesh needs an adequate interdisciplinary policy guideline and political wills to implement it for sustainable management and protection of wetlands, and ecologically sensitive sites (Islam, 2010). Tanguar Haor's directly used resources are easier to quantify than the other types of benefits, although, because of lack of reliable data, much of this will have to be inferred or estimated (Ali, 2014).

So, in depth study about the changing pattern of the productive landscape and the impact of such change is a growing need to uphold the natural biodiversity of the region. Geospatial technology (GIS, RS) used in this study to signify the importance of land cover changes over the Haor basin, which possibly help to assess

the change dynamics of the area. Scientific change assessment may also help the policymakers to understand the natural state of the area and the complex relation between the physiographic and man-made features.

2. Study area

Tanguar Haor is located in the northeastern part of Bangladesh, between $25^{\circ} 12' 2.572''$ and $25^{\circ} 5' 47.989''$ North Latitude and $90^{\circ} 58' 49.426''$ and $91^{\circ} 10' 0.018''$ East Longitude. The total area of Tanguar Haor is approximately 160 square kilometers including all Geographic features and land cover. It shares a border of approximately 17 km with Nongstoin (Meghalaya), India in its north. The Haor is almost 2.5 km away from neighboring Netrakona district in the west. Tanguar Haor possesses 88 villages. Fig. 1 shows the location of Tanguar haor and its surroundings.

The haor is located at an altitude of only 2.5–5.5 m above mean sea level. The landscape topography of Tanguar Haor is uneven. Because of its bowl shape nature, it acts like a natural reservoir. The Haor consist of 46–50 beels of various sizes (BFD, 2012). Within 160 square kilometers 2802.36 ha is permanent waterbodies (Banglapedia, 2006). Total river area within the Tanguar Haor is 359.39 ha (Sobhan et al., 2012). Tanguar Haor act as the flood plain complex of Surma-Kushiyara river system. These two rivers are important tributaries of Meghna River and also connected with Dhanu, Baulai and Jadukata River through the extended floodplain of Tanguar Haor.

3. Materials and methods

3.1. Data collection

The present study is in view of both primary and secondary information. The primary information was gathered through the poll review, organized and unstructured meeting with key witnesses, direct field perception and dialogs with the common individuals of the study area. On the other hand, the preliminary secondary data for this study was collected from free available satellite image archives, other secondary data sources include various non-governmental organization, distributed and unpublished sources, for example, reports, articles, diaries, day by day daily papers, records, maps etc.

3.1.1. Primary data collection

3.1.1.1. Reconnaissance survey. Reconnaissance survey was done at the starting level of the study. Firstly, boundary was delineated by available map resources to understand the extent of the study. A short field observation for primary documentation was done. Under the primary observation field introduction, objectives identification, previous survey evidence query, scope identification was instituted.

3.1.1.2. Field survey. Though the whole study was based upon available secondary data, a short field survey was conducted for proper validation of available data. Field survey also helped to understand the natural sitting of the study area as well as to understand the perception of the local people relevant to this study.

3.1.1.3. Interview. Short interview of the local people specially the older ones was conducted to understand their perception about the trends of Land cover. Informal interview also helps to understand their adaptive nature and resource consumption strategy.

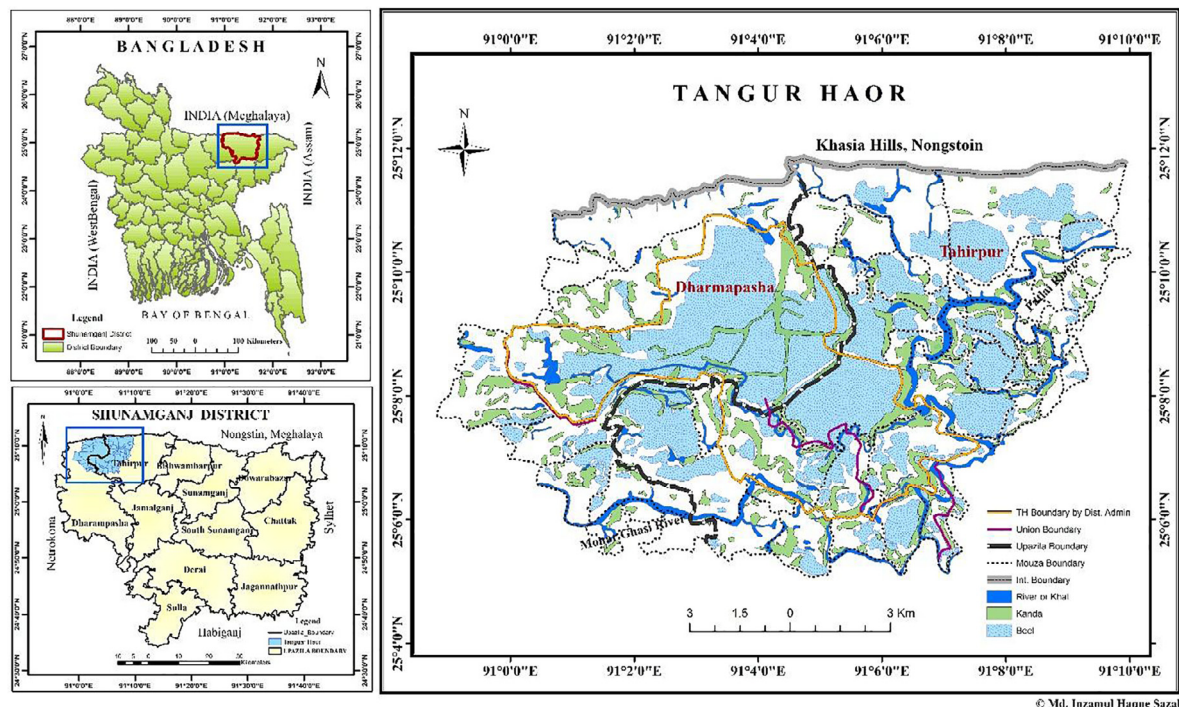


Fig. 1. Location of Tanguar Haor.

3.1.2. Secondary data collection

3.1.2.1. Base map collection. Base maps for this study include Tanguar Haor Area map, Mouza map, Union map, Upazilla map and available land use map of the study area. Main Base map was collected from Community Based Sustainable Management of Tanguar Haor Program by the GoB. Two different boundary of Tanguar Haor was found, one from Local administration of Sunamganj and another proposed by IUCN & CNRS. After collection, an overlay analysis was done to understand the relativity of the two-delineated area. Mouza shape file was collected from a free-ware GIS data sources Geo Planning for Advanced Development in Bangladesh (GPADBD).

3.1.2.2. Satellite data acquisition. To analyze 30-year land cover change four Landsat satellite image of 1980, 1989, 2001 and 2010 was downloaded from United States Geological Survey (USGS) official website (earthexplorer.usgs.gov). Every satellite imagery represents the dry season and Landsat MS, TM and ETM sensor data were taken in count (Table 1).

3.2. Data analysis

The total analysis was based on transforming ideas into maps and graphs. Temporal Satellite dataset from 1980 to 2010 were analyzed individually. A short generalization was done for proper planning. After the analysis of each satellite data the results were compared to evaluate the study findings. A detail change detection analysis was assessed by implementing pre-and post-change detection techniques. Integration of several techniques identified

the critical change areas. The whole analysis procedure was performed following the underlying flowchart (Fig. 2).

3.3. Result evaluation and report writing

The study focuses on the land cover change over a long period (1980–2010) of the study area. So, the overall scientific analysis determined the state, dynamics, and trend of changing landscape of Tanguar Haor. Besides the change detection the relation and interaction between various land cover was also assessed. The overall scenario of changing land cover was evaluated with satisfactory precision.

4. Result and discussion

4.1. Preprocessing

4.1.1. Noise reduction

Common forms of noise include systematic striping or banding and dropped lines. The overall appearance was thus a ‘striped’ effect (Jacqueline, NASA). Discrete Fourier Transform (DFT) method was used to reduce the noise from 1978 image. The quantity of frequencies compares to the quantity of pixels in the spatial space picture, i.e. the picture in the spatial and Fourier space is of the same size. For a square image of size $N \times N$, the two-dimensional DFT is given by the following equation.

$$F(k, l) = \sum_{i=0}^{N-1} \sum_{j=0}^{N-1} f(i, j) e^{-j2\pi \left(\frac{ki}{N} + \frac{l}{N} \right)}$$

Table 1

Details of acquired satellite images.

Satellite id	Sensor id	Path/row	Acquisition date	Spatial resolution	Quality
Landsat 3	MSS	147/43	02-02-1980	60 m	0
Landsat 4	TM	137/43	28-01-1989	30 m	9
Landsat 7	ETM	137/43	29-01-2001	30 m	9
Landsat 5	TM	137/43	30-01-2010	30 m	9

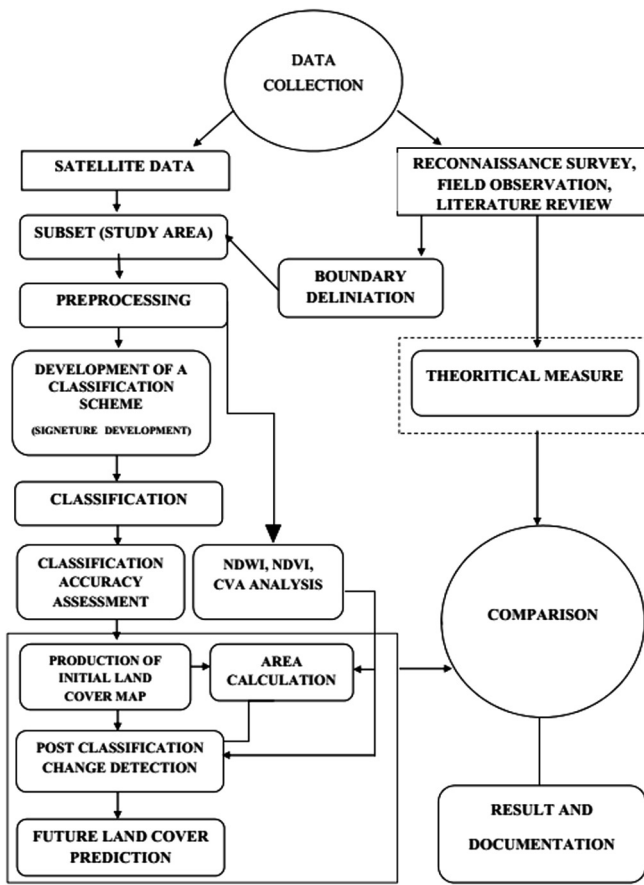


Fig. 2. Data analysis flowchart.

where $f(i,j)$ is the image in the spatial domain and the exponential term is the basis function corresponding to each point $F(k,l)$ in the Fourier space. The satellite image of 1980 includes some of this stripped effect. The band 4 among the all bands contained excessive noise. The noise was reduced at a level via Fourier analysis shown in Fig. 3.

4.1.2. Radiometric calibration

Radiometric characterization and calibration is a prerequisite for creating high-quality science data, and consequently, higher-level downstream products (Chander et al., 2009). Landsat Satellite sensors capture images of Land cover as Digital Number (DN) value

rather than Top of Atmosphere (ToA) reflectance units. The main purpose of this step was to convert the digital numbers to Top of Atmosphere reflectance units. Equations and parameters to convert calibrated Digital Numbers (DNs) to physical units, such as at-sensor radiance or Top-Of-Atmosphere (TOA) reflectance, have been presented in a “sensor-specific” manner elsewhere, e.g., MSS (Markham and Barker, 1987), TM (Chander and Markham, 2003), ETM + (Handbook2), and ALI (Markham et al., 2004). Different calibration values differ according to sensor id and acquisition date. Total calibration procedures consist of two steps, the first one was Converting DN(Q_{cal}) to Radiance (L_λ) and the second one was Converting Radiance (L_λ) to Reflectance (ρ_λ).

$$L_\lambda = \left(\frac{L_{MAX_\lambda} - L_{MIN_\lambda}}{Q_{calmax} - Q_{calmin}} \right) (Q_{calmax} - Q_{calmin}) + L_{MIN_\lambda}$$

Or,

$$L_\lambda = G_{rescale} \times Q_{cal} + B_{rescale}$$

where,

$$G_{rescale} = \left(\frac{L_{MAX_\lambda} - L_{MIN_\lambda}}{Q_{calmax} - Q_{calmin}} \right); B_{rescale} \\ = L_{MIN_\lambda} - \left(\frac{L_{MAX_\lambda} - L_{MIN_\lambda}}{Q_{calmax} - Q_{calmin}} \right) Q_{calmin}$$

Conversion from Q_{cal} in Level 1 products back to at-sensor spectral radiance (L_λ) requires knowledge of the lower and upper limit of the original rescaling factors (Chander et al., 2009). During radiometric calibration, pixel values (Q) from raw, unprocessed image data were converted to units of absolute spectral radiance using 32-bit floating-point calculations. The absolute radiance values were then scaled to 7-bit (MSS, $Q_{calmax} = 255$), 8-bit (TM and ETM+, $Q_{calmax} = 255$), and 16-bit (ALI, $Q_{calmax} = 32,767$) numbers representing Q_{cal} before layout.

The second step of radiometric calibration operation was to convert the sensor spectral radiance (L_λ) to Top of Atmosphere (TOA) reflectance. When comparing images from different sensors, there are three advantages to using TOA reflectance instead of at-sensor spectral radiance. First, it removes the cosine effect of different solar zenith angles due to the time difference between data acquisitions. Second, TOA reflectance compensates for different values of the exoatmospheric solar irradiance arising from spectral band differences. Third, the TOA reflectance corrects for the variation in the Earth-Sun distance between different data acquisition dates.

$$\rho_\lambda = \frac{\pi L_\lambda d^2}{ESUN_\lambda \cdot \cos\theta_s}$$

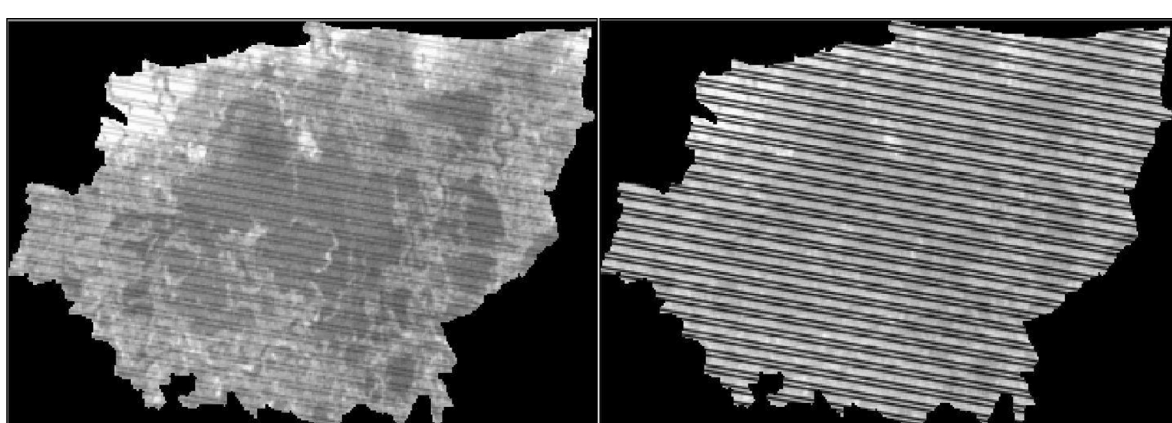


Fig. 3. Noise reduction before image (left), after image (right).

ρ_λ = Planetary TOA reflectance [unitless]; π = Mathematical constant equal to ~ 3.14159 [unitless]; L_λ = Spectral radiance at the sensor's aperture [$W/(m^2 \text{ sr } \mu\text{m})$]; d = Earth–Sun distance [astronomical units]; $ESUN_\lambda$ = Mean exoatmospheric solar irradiance [$W/(m^2 \mu\text{m})$].

A manual Radiance to reflectance model was constructed to measure TOA reflectance value of each bands. Earth sun distance value was collected from Julian Day Calendar. The value of exoatmospheric solar irradiance was summarized for the MSS, TM, ETM+, and ALI sensors using the Thuillier solar spectrum (Thuillier et al., 2003). Fig. 4 presented an example of radiometric calibration of Landsat 7 ETM+ image, (acquisition date: 29-01-2001, band: 4) via systematic modelling which visualize the effective process of conversion of Spectral Radiance into TOA reflectance.

4.2. Classification

The Supervised Maximum Likelihood classification used in this study is the most common method in remote sensing image data analysis (Richards, 1995). It identifies and locates land cover types that are known a priori through a combination of personal experience, interpretation of aerial photography, map analysis and field-work (Jensen, 2005). It uses the means and variances of the training data to estimate the probability that a pixel is a member of a class. The pixel is then placed in the class with the highest probability of membership (Ozesmi and Bauer, 2002).

A classification scheme was developed for further analysis of the images, based on the characteristics of the area (Table 2). Tanguar Haor is bounded mostly by water and vegetation. Some settlements shown in the upper and lower corner of the images.

Bare land was included in the settlement class during the development of the classification scheme. As Tanguar Haor is mostly covered by wetlands of different sizes and depths, the inundated sites were classified into two detail classes e.g. deep water and shallow water.

After development of signature file, the final step was image classification. Maximum likelihood parametric rule was applied during classification as mentioned before. Based on statistics (mean; variance/covariance), a (Bayesian) Probability Function was calculated from the inputs for classes established from training sites. Each pixel was then judged as to the class to which its most probably belong (Fig. 5).

4.3. Accuracy assessment

In this study classification accuracy assessment was conducted with the reference of the raw satellite images. In maximum likelihood classification, often many pixels remain misclassified because of the uneven distribution of data. Classification accuracy should be done by ground truthing, or by physical appearance in the study site. But in these case time is one of the major resistant because you can't measure the past with the present. So, to acquire better accuracy of the classification both infield and outfield accuracy assessment is necessary. In this study outfield assessment was done by random sampling of the reference image. The total process was done by comparing the reference image with the classified image with some random points. Stratified random sampling was adopted to calculate the classification accuracy of each land cover image. The logic to use this sampling method is- each land cover class found equal probability to be observed. 50 Random points

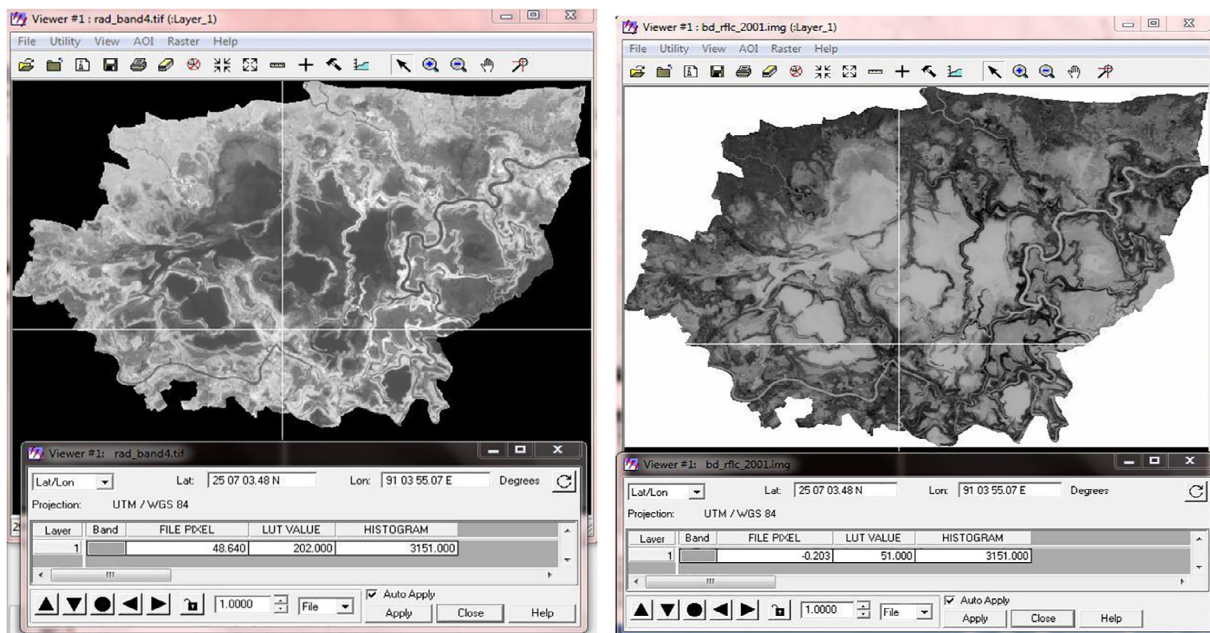


Fig. 4. Radiometric calibration in Erdas imagine-input image L_λ (left), output image ρ_λ (right).

Table 2

A detail classification scheme used for supervised classification.

Code	Land cover types	Description
1	Deep Water	River, permanent open water, perennial lakes and reservoirs
2	Vegetation	High land agriculture, forest, trees, shrub lands
3	Shallow Water	Semi inundated land filled with marshy vegetation
4	Settlement	Temporary and permanent houses, villages, artificial infrastructure, roads

CLASSIFIED LAND COVER MAPS OF TANGUAR HAOR

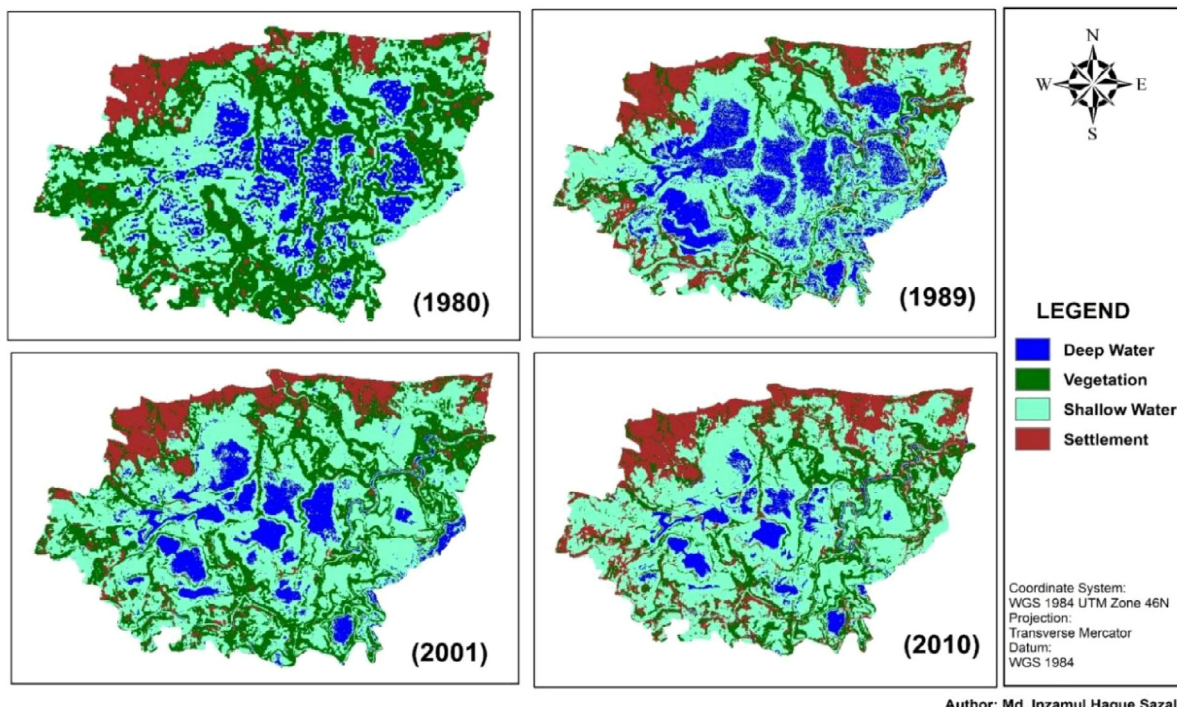


Fig. 5. Classified land cover maps of Tanguar Haor (1980–2010).

were used for accuracy assessment of every classified image. Some observation show “0” class values, which are neglected. The data is summarized and quantified by using error matrix. Four different accuracy results- user accuracy, producer accuracy, total accuracy, kappa index was produced from the overall assessment which help to understand the accuracy of the classification.

The calculated assessment result of each classified satellite image from 1980 to 2010 was shown from [Tables 3–6](#). Calculated total accuracy result for each satellite image (1980, 1989, 2001, 2010) given as 73.91%, 80.49%, 91.30% and 89.13% respectively, when calculated kappa statistics results are 0.6548, 0.7273, 0.8837 and 0.8543 respectively derived from [Tables 3–6](#).

Table 3
Accuracy Assessment result of classified image (02-02-1980).

Class names	Reference totals	Classified totals	No. correct	Producers accuracy	User accuracy	Conditional kappa for each category
Deep water	11	10	10	90.91%	100%	1.0000
Vegetation	7	13	6	85.71%	46.15%	0.3649
Shallow water	12	13	8	66.67%	61.54%	0.4796
Settlement	16	10	10	62.50%	100%	1.0000
Totals	46	46	34			

Table 4
Accuracy assessment result of classified image (28-01-1989).

Class names	Reference totals	Classified totals	No. correct	Producers accuracy	User accuracy	Conditional kappa for each category
Deep water	11	8	8	72.73%	100%	1.0000
Vegetation	9	6	6	66.67%	100%	1.0000
Shallow water	14	21	14	100%	66.67%	0.4938
Settlement	7	6	5	71.43%	83.33%	0.7990
Totals	41	41	33			

Table 5
Accuracy assessment result of classified image (29-01-2001).

Class names	Reference totals	Classified totals	No. correct	Producers accuracy	User accuracy	Conditional kappa for each category
Deep water	11	10	10	90.91%	100%	1.0000
Vegetation	11	12	11	100.00%	91.67%	0.8905
Shallow water	13	14	12	92.31%	85.71%	0.8009
Settlement	11	10	9	81.82%	90.00%	0.8646
Totals	46	46	42			

Table 6

Accuracy assessment result of classified image (30-01-2010).

Class names	Reference totals	Classified totals	No. correct	Producers accuracy	User accuracy	Conditional kappa for each category
Deep water	11	10	10	90.91%	100%	1.0000
Vegetation	10	11	9	90.00%	81.82%	0.7677
Shallow water	14	14	13	92.86%	92.86%	0.8973
Settlement	11	11	9	81.82%	81.82%	0.7610
Totals	46	46	41			

The highest classification accuracy was found in case 2001 image, which was a product of Landsat ETM + sensor. All other images were either the product of Landsat TM sensor or oldest MSS sensor. So, it is a clear indication that accuracy of a classification highly dependent on the version of satellite dataset. More advance version produces more accurate result. Almost all the evaluated result shows satisfactory value except the classified image of 1980 yet accepted.

4.4. Land cover change detection

There are two broad methods of Change Detection Techniques includes- a) Pre-Classification Method, b) Post Classification Method. Pre-Classification method analyses the change without classifying the image value. The most common and widely used pre-classification method is "Vegetation Index Differencing (NDVI)". Various index has developed after NDVI e.g. NDWI, MNDWI, Change Vector Analysis (CVA) etc. On the other hand, post Classification method is the most widely used change detection method of modern times. Post classification evaluate the change in land cover based on a detail categorized classification of land cover. Post Classification comparison, Aerial Difference calculation, Image Differencing, Image rationing, Image regression etc. are

some of the common post classification Change detection approaches.

4.4.1. NDVI analysis

NDVI is calculated on a per-pixel basis as the normalized difference between the red and near infrared bands from an image:

$$\text{NDVI} = \frac{\text{NIR} - \text{RED}}{\text{NIR} + \text{RED}}$$

where NIR is the near infrared band value for a cell and RED is the red band value for the cell. NDVI value ranges from "+1 to -1". Close to '+1' means denser and greener vegetation and close to '0' means less green or other colored vegetation or dry leaf. '0' means no vegetation and '0 to -1' represent other land cover types. For Landsat TM and ETM sensors band 4 is regarded as NIR and Band 3 regarded as RED. But in case of the acquired image of 1980 consist of the oldest MSS sensor, it's hard to identify specific bands for NDVI analysis. This Study use band 5 as RED and band 6 as NIR to evaluate the vegetation differentiating. The output NDVI maps were shown in the left side and the classified NDVI maps were shown in the right side (Fig. 6). After successful production of NDVI maps unsupervised classification techniques was used to classify the resultant dataset. Iso-data algorithms with Maximum iteration 6 and Convergence Threshold 0.950 used to classify each Vegetation Differentiating

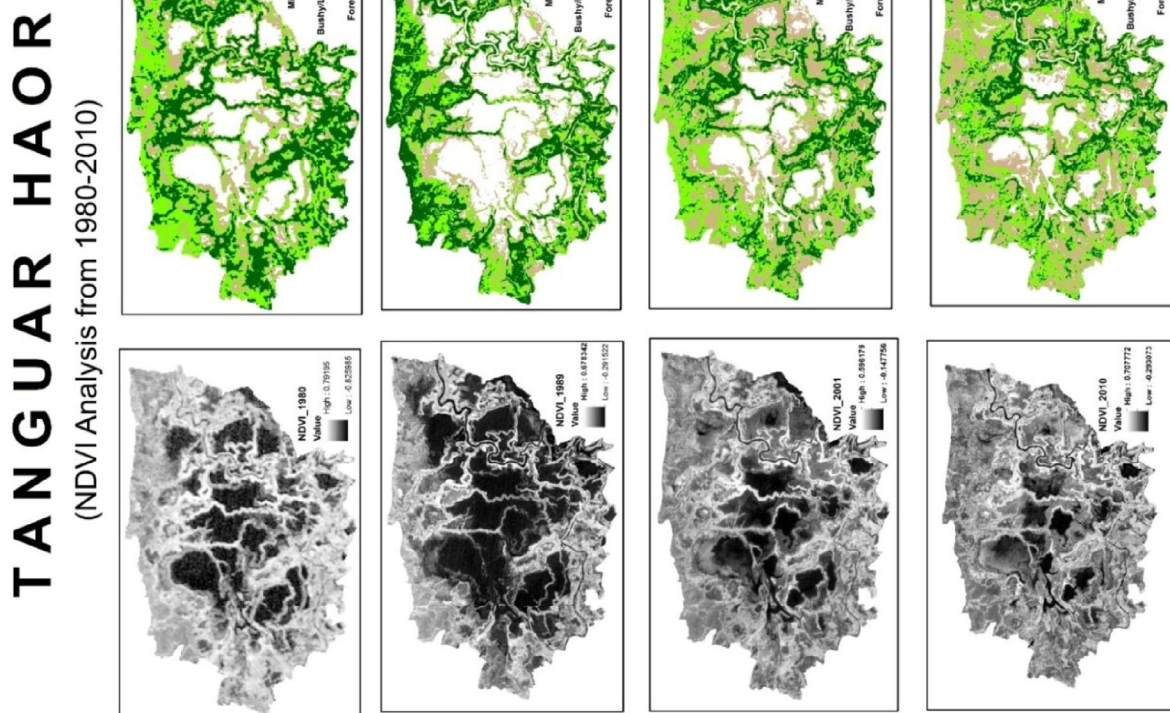


Fig. 6. Vegetation differentiating (NDVI) analysis of Tanguar Haor (1980–2010).

Image. Only positive values were taken in count to classify each image. Higher positive values are classified as forested vegetation and values close to zero are classified as mix vegetation which might consist of settlement, water body, or any other land cover feature. All the negative value including zero are classified with default legend and then ignored during presentation. After aerial calculation of classified NDVI images (Fig. 6) linear regression line was constructed for each category (Fig. 7). Time was taken as the independent factor (x) and area was taken as the dependent factor during the calculation.

A significant decline in forested high land vegetation; a significant incline in Mix vegetation consist of various anthropogenic elements e.g. settlement; and a moderate incline in Bushy or low land vegetation includes crop fields, marshy vegetation was shown in Fig. 7.

4.4.2. NDWI analysis

The normalized difference water index (NDWI) is derived using similar principles to the Normalized Difference Vegetation Index (NDVI). If the equation is reversed and the green band used instead of the red, then the outcome would also be reversed, the vegetation suppressed and the open water features enhanced (McFeeters, 1996). The equation is as follows:

$$CM = \sqrt{(DN_{11} - DN_{21})^2 + (DN_{12} - DN_{22})^2 + (DN_{13} - DN_{23})^2 + (DN_{14} - DN_{24})^2}$$

$$NDWI = GREEN - NIR/GREEN + NIR$$

For Landsat TM and ETM sensors band 2 was regarded as GREEN and Band 4 regarded as NIR but in case of the acquired image of 1980 consist of the oldest Landsat MSS 3 sensor, this Study used band 4 as GREEN and band 6 as NIR to delineate water differentiating index.

Fig. 8 demarcated the NDWI analysis result for every respective year from 1980 to 2010. The Grayscale images in the left side shows the NDWI values. Higher values indicate the water extent and lower values demarcate other land covers. In the right side 4 consecutive maps are produced based on the NDWI values. Only higher positive NDWI values are taken to classify two water

classes. Unsupervised classification approach used to classify the NDWI dataset.

After classification and aerial calculation, a linear regression (Fig. 9) was implemented which results a downward trend line for the deep water class when a positive increase found in case of Shallow Water class. Time was taken as the independent factor (x) and Area was taken as the dependent factor during the calculation.

4.4.3. CVA analysis

A change vector is the difference vector between two vectors in n-dimensional feature space defined for two observations of the same geographical location (i.e. corresponding pixels) during two dates (Nackaerts et al., 2005). The Study had taken 8 bands comprised of 2 bands for each year (1980, 1989, 2001, 2010). RED and NIR channels for each date were taken for the analysis (Table 7). As the raster bands of 1980 comprised of different values and pixel components, band 5 and 6 are taken as the RED and NIR bands. To CVA analysis with raster bands of 1980, principle component analysis executed to segregate noise components and to normalize the band images (band 5 and band 6) to 30 m.

For two dates and four bands magnitude of change calculated by as follows:

where DN_{ij} is the digital number recorded in band j for date i.

This study delineated Change magnitude (CM) value for Tangar Haor from 1980 to 2010 in three time spans (Fig. 10). Firstly, total CM value was assessed by computing 1980 and 2010 images (Fig. 10a). The magnitude value shows some unusual results due to the characteristic difference between MSS (1980) and TM (2010) image. Then CM for 20 years (1989–2010) was evaluated (Fig. 10b). Finally, CM value between 1989–2001 (Fig. 10c) and 2001–2010 was calculated (Fig. 10d).

Fig. 10a stated that, around 50% of the total landscape of Tangar Haor has been changed or shifted within 30 years. The most gradual changes taken place in the middle part consist of various

Areal Extent and Trend of Vegetation Cover

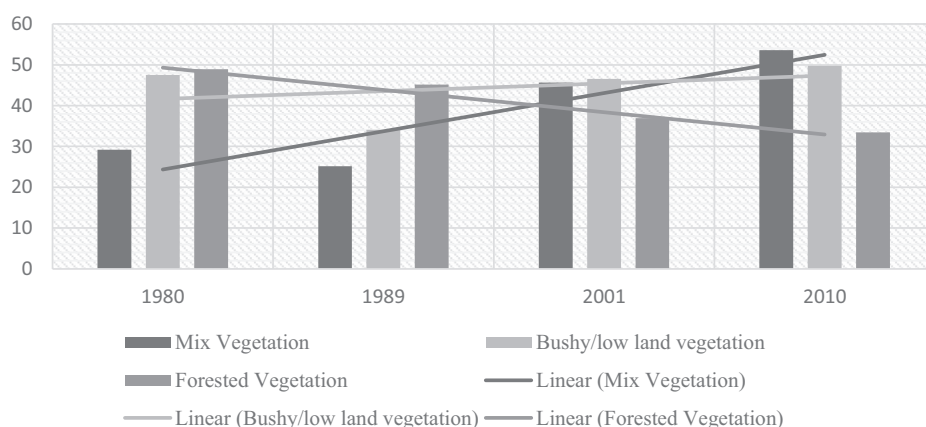


Fig. 7. Change in vegetation cover of Tangar Haor (sq. km).

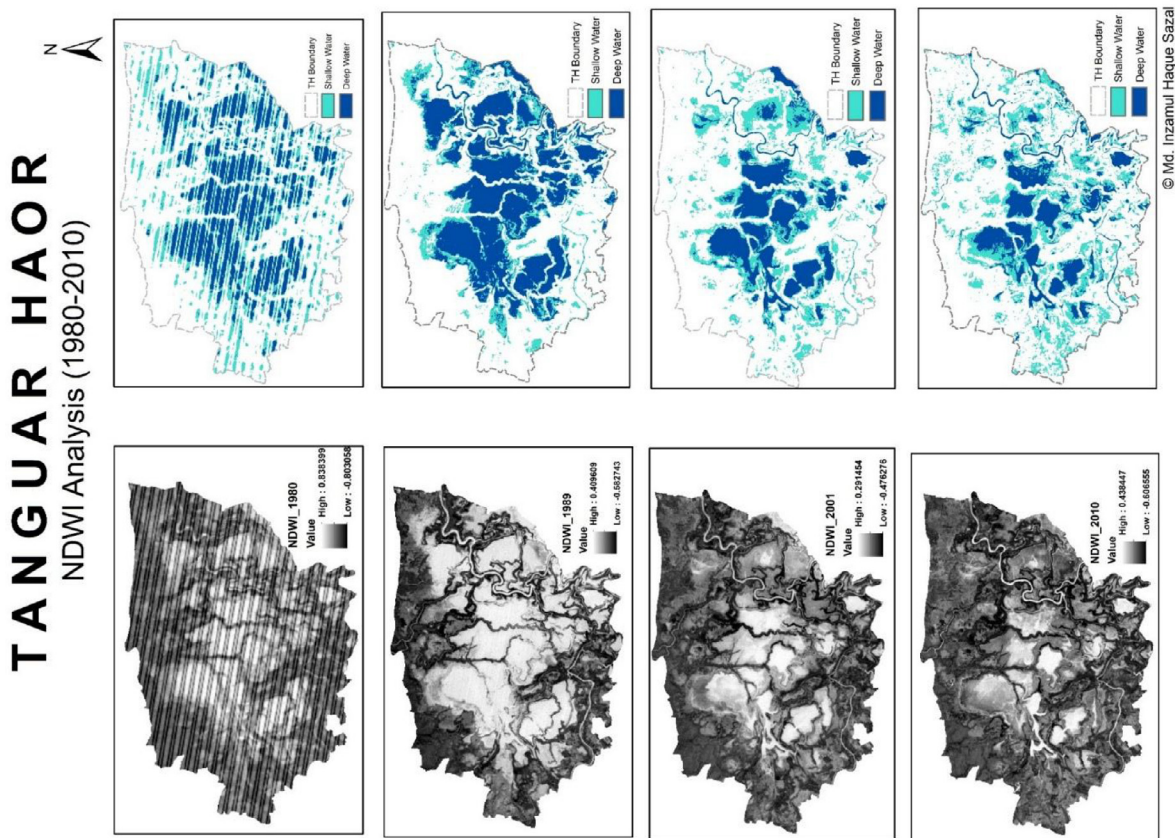


Fig. 8. Water differentiating (NDWI) analysis of Tanguar Haor (1980–2010).

Areal Extent and Trend of Water Cover

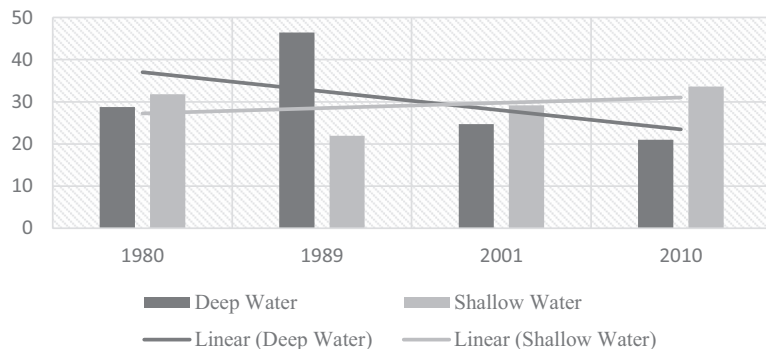


Fig. 9. Change in water cover (sq. kms).

Table 7

Pair of datasets taken for change vector analysis.

Change between				CVA	
Earlier date	Bands taken	Later date	Bands taken	Direction	Magnitude
1980	5,6	2010	3,4		↖
1989	3,4	2001	3,4	↖	↖
1989	3,4	2001	3,4	↖	↖
2001	3,4	2010	3,4	↖	↖

beels. The upper part shows lower magnitude of change and the south-eastern part shows a moderate change.

Magnitude of change between 1989 and 2010 (Fig. 10b) shows a moderate change scenario. The change values fluctuate between

0.02 and 0.26. There are very few areas with rapid change. The rate of change continued between 1989 and 2001 shown in Fig. 10c.

Tanguar Haor experienced a dramatic change in recent years between 2001 and 2010 (Fig. 10d). Most interesting thing was that,

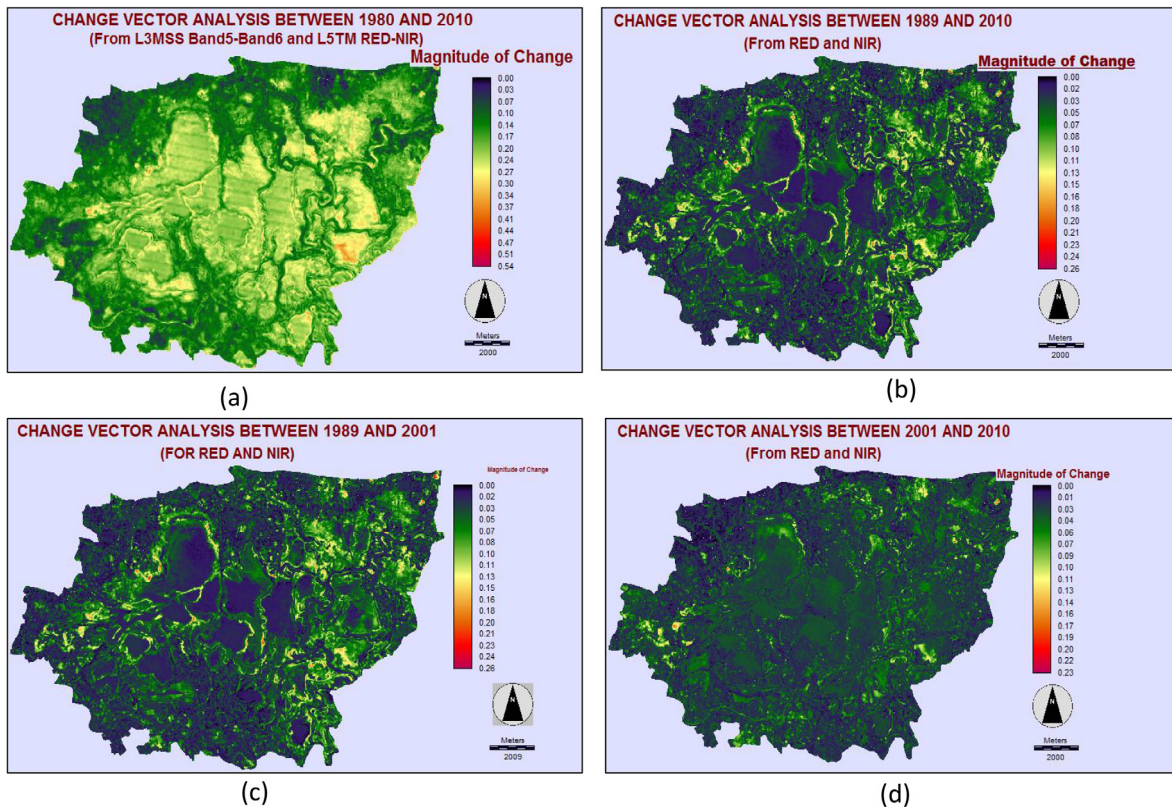


Fig. 10. Graphical representation of CVA showing the magnitude of change.

almost the whole Tanguar Haor experiences an average change. Magnitude of change was little lower than the previous years but the changes became more diverse and frequent.

The second output image (Fig. 11) contains information about the direction of the change event in spectral feature space. The change vector direction is presented in the form of a code, referring to the multi-dimensional sector in which the change vector occurs (Jensen, 2005). Firstly, A text output was produced to provide a key describing sector codes, relating the change vector to positive or negative shifts in n-dimensional feature space. The vector direction files are processed in ArcGIS platform for expected outcome. The output direction files are firstly classified into for distinct classes to assess the change group. After that two similar CVA direction image overlaid, from which one was showing the Change class and another one was showing the Vector Field Symbology. Both the magnitude component and the direction component was inputted, vector average thinning method was used to calculate the contiguity, each symbol (Single Arrow) scaled to 1000 m/arrow and geographic reference system with from angle was used to calculate the geometric arrangement.

4.4.4. Change detection statistics

Its a statistical technique used to compile a detailed tabulation of changes between two classification images. The analysis identifies the classes into which those pixels changed in the final state image. This technique also provides an in-depth idea about pixel transformation and class change which provide an in-depth idea about the dynamics of converted landscapes. This study used ENVI 5.1 software platform to execute change detection statistics. ENVI visualize the statistics of land cover change in a set of transition matrix. ENVI uses the available map information to automatically coregister the images.

No resampling had done before calculation, so the images may carry some error, but as the images are strongly uncorrelated

resampling error were negligible. The statistics tables listed the initial state classes in the columns and the final state classes in the rows. However, the columns include only the selected (paired) initial state classes, while the rows contain all the final state classes (Tables 8, 9).

Both the tables explained the total change scenario between past and present time with the transformation statistics of each class. Example – in case of Settlement class around 77% of initial settlement (1980) remain the same class in the final state (2010). Moreover 21% of vegetation converted into settlement in the final state and approximately 13% of shallow water changed to settlement in the final state. The image difference row shows the direction or behavior of change. Negative values indicates decrease and positive values indicates increase in land cover feature.

4.4.5. Thematic change dynamics

A convenient way to assess the post classification change dynamics is identifying the thematic change based on change statistics. ENVI thematic change workflow tool was used to portray the dynamics of land cover change that have taken place in Tanguar Haor from 1980 to 2010. The tool measures the transition dynamics of a land cover class to another class at a given extent. Firstly, initial state image was inputted as a time 1 image and final state image as time 2. Image registration task was skipped as done before during area calculation. Only changed areas were taken to visualize the overall dynamics. Total 24 unique classes were introduced as a change factor between the two-time span. The study only considered the valid classes which carry a significant change resultant. 13 classes were eliminated as they have no valid change or '0' change value to visualize. After the execution, an optional clean-up or Refine operation was done to strengthen the output. Smooth Kernel Size was specified as 3×3 pixel. The square kernel's centre pixel will be replaced with the majority class value of the kernel. At the final stage three distinct output file was cre-

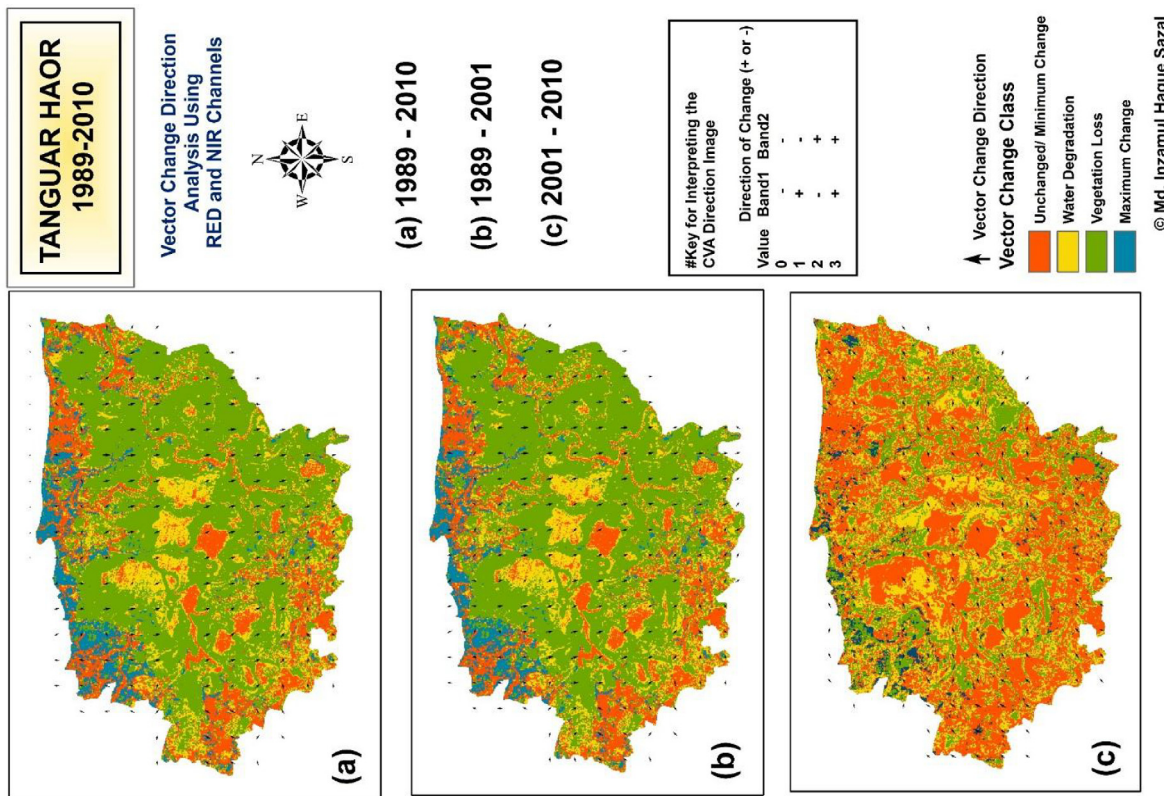


Fig. 11. CVA direction images of Tanguar Haor.

Table 8

Statistical table showing the change percentage of Tanguar Haor from 1980 to 2010.

Initial state (1980) Percentages (%)	Final state (2010)	Deep water	Vegetation	Shallow water	Settlement	Row total	Class total
Deep water	28.707	0.397	6.175	0	99.964	100	
Vegetation	0.613	35.768	7.473	13.542	99.748	100	
Shallow water	69.825	41.766	73.327	4.304	99.816	100	
Settlement	0.836	21.34	12.586	77.357	99.795	100	
Class total	100	100	100	100	0	0	
Class change	71.293	64.232	26.673	22.643	0	0	
Image diff	-49.071	-52.899	33.582	140.789	0	0	

Table 9

Statistical table showing the aerial change of Tanguar Haor from 1980 to 2010.

Initial state (1980) Area (sq. m.)	Final state (2010)	Deep water	Vegetation	Shallow water	Settlement	Row total	Class total
Deep water	5.562	0.2412	4.0608	0	9.864	9.8676	
Vegetation	0.1188	21.7224	4.914	1.7784	28.5336	28.6056	
Shallow water	13.5288	25.3656	48.2184	0.5652	87.678	87.84	
Settlement	0.162	12.96	8.2764	10.1592	31.5576	31.6224	
Class total	19.3752	60.732	65.7576	13.1328	0	0	
Class change	13.8132	39.0096	17.5392	2.9736	0	0	
Image diff	-9.5076	-32.1264	22.0824	18.4896	0	0	

ated from which the first one is thematic change image (Fig. 12), second one is thematic change vector file and the final output consist of thematic change statistics (Table 10).

Fig. 12 was the thematic change workflow output of Table 10 which concluded that, the highest amount of land cover conversion had taken place from vegetation to shallow water (14%). This con-

version rate was highest between 1980 and 1989 and lowest between 2001 and 2010. The conversion rate from deep water to shallow water and vegetation to settlement was almost same in 30 years. A small amount of change had taken place from Shallow water to (settlement, deep water and vegetation). Other changes or conversions were below 1% hence neglected.

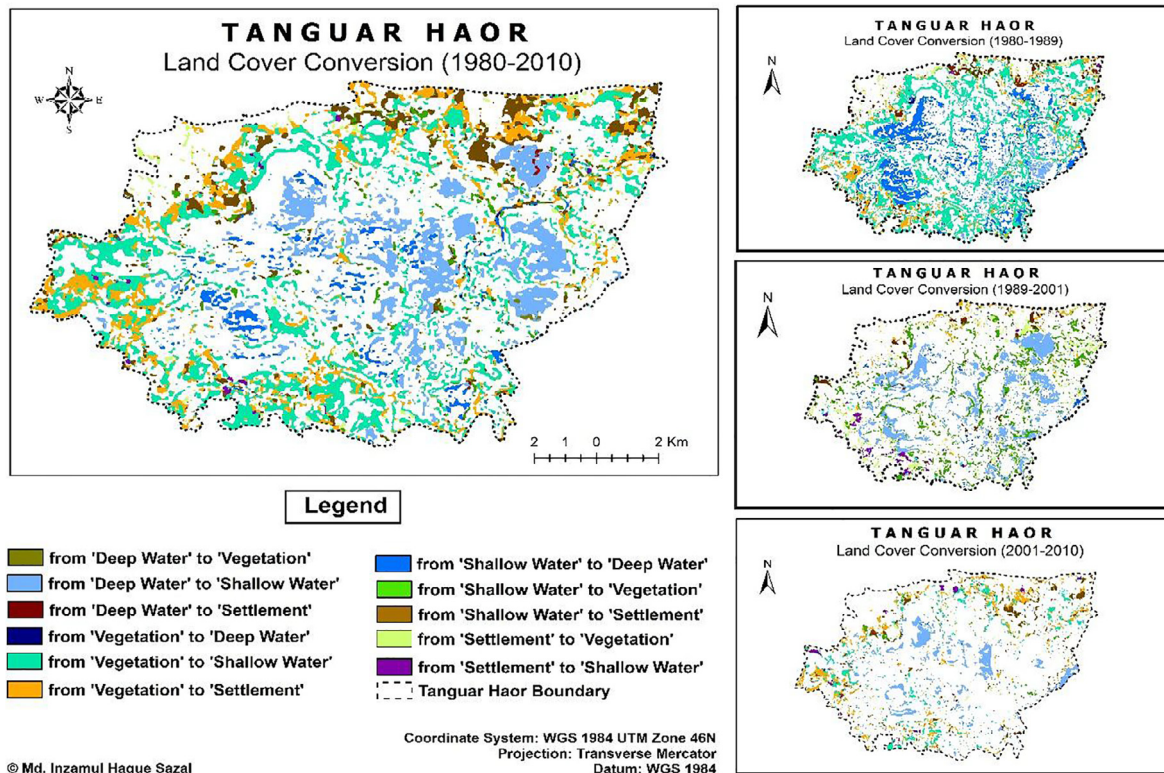


Fig. 12. Resultant output of thematic change workflow analysis (1980–2010).

Table 10

Resultant thematic change statistics: from-to change matrices (1980–2010).

1980	2010	Changed area (sq. km)	Percent change
From deep water	To vegetation	0.94500	0.0590625
From deep water	To shallow water	12.989700	8.1185625
From deep water	To Settlement	0.104400	0.06525
From vegetation	To deep water	0.81000	0.050625
From vegetation	To Shallow Water	22.464000	14.04
From vegetation	To settlement	11.402100	7.1263125
From shallow water	To deep water	3.289500	2.0559375
From shallow water	To vegetation	2.160900	1.3505625
From shallow water	To settlement	6.342300	3.9639375
From settlement	To vegetation	1.259100	0.7869375
From settlement	To shallow water	0.425700	0.2660625

4.5. Discussion on land cover change detection analysis

Different pre and post classification methods were used in this study for complete identification and in depth analysis of land cover change. Each method produce different types of results which helps to analyze the complex behavior of land cover feature.

As vegetation and water are the most common feature of the study area, to demarcate the identical change between the variables of vegetation cover or water body NDVI and NDWI analysis was taken place. By the implementation of NDVI and NDWI analysis an in-detail classification of vegetation cover e.g. marshy vegetation, high land vegetation etc. as well as water cover was presented. As a pre-classification method NDVI and NDWI helped to accurately identify the vegetation and water body respectively. After unsupervised classification of NDVI images the most threatened vegetation cover (forested vegetation) was identified.

CVA analysis graphically demarcate the magnitude and direction of land cover change, which helps to rectify the most

threatened sites and the behavior of change around the study area.

Being a post classification method change detection statistics quantified the amount of change in each land cover types. The results of image differencing concluded the increasing trend of shallow water (33%) and settlement class (140%) and decreasing trend of deep water (49%) and vegetation cover (52%). This analysis also helps to understand the amount of unchanged land cover with remarkable precision.

Thematic change workflow finally helped to visualize the typical dynamics of the changing land cover within different time periods. As a fundamental function, transition probability matrix signifies the "form – to" matrix which exemplify the past and present state of different land cover. This analysis also justified the typical behavior of each land cover types considering the change dynamics.

Integration of all above mentioned techniques helped to understand the magnitude, state, direction, and dynamics of land cover

change in several possible prospects. But there had some issues with both pre and post classification change detection techniques. Most of the pre-classification techniques identify the change result only considering the change or variation in reflectance value without classifying the land cover. The operator need to be much intellectual, experienced, and identical to justify and signify the change. On the other hand, post classification analysis is quite flexible to handle and easy to quantify the statistics of change class. But accuracy is a prime concern in this case, as mislead in classification scheme can lead to numeric errors.

5. Conclusion

Impact of land cover change influence approximately 40% of the total landscape of the study area within 1980 to 2010. The overall analysis found that over anthropogenic influence was the major cause behind the change. The result shows that 71% extent of deep water body change its state mostly to shallow water. The NDWI analysis shows around 25.4583 square kilometer of deep water body has degraded within 1989–2010. According to the local people rice cultivation becoming more popular than fishing specially in the dry season which accelerates the rate of degradation of deep water.

Once high land vegetation or forested vegetation was the second dominating land cover feature of Tanguar Haor. But within 30 years from 1980 it is decreased more than 50%. The transition matrix shows that; the forested vegetation land was either transferred to shallow water or settlement. The NDVI analysis evaluate a more precise result. Around 15.9967 square kilometer of forested vegetation land has degraded in 30 years from 1980. The acceleration of degradation was maximum within 1989–2001 (12.4902 sq. km) when most of the forested land was transferred to semi emergent crop land. Popularity of crop cultivation and hence emergence of settlement is the main culprit behind such clear cutting of emergent forested trees.

The change statistics shows that the shallow water body increased by 33% in 30 years. As the shallow water is more friendly for agricultural activities, overabundance of shallow water encourage the local people to build semi-permanent or permanent settlement which resultant a serious damage to the haor ecosystem e.g. fish diversity.

According to image difference statistics settlement feature inclined by 140% within the study period which imposes serious threat to other land features. Population pressure and insufficient land is the main cause of settlement expansion in the adjacent area of Haor Basin. The doubling rate of settlement is only 20–25 year. In the past settlement was condensed only in the upper and lower corner of the Haor Basin but at present time the feature seems to be dominated extensively all over study area.

In field study found that- very few people are like to live in the adjacent Haor area because of seasonal calamities e.g. flood. But the overwhelming population pressure push the poor to live in the hostile land as the land is cheap and free for economic activities. Every one of the local community confess about the degradation of land cover features of Tanguar Haor but they never know the causes and consequences of such alarming degradation. They never think about the future or learned from the past, they are only depending on present. They only aware of how to consume and how to gain self-sufficiency. So, capacity building by different training activities under an integrated conservation plan is the precautionary step of land conservation. If people able to learn how much to consume and what to consume, the natural balance will be restored and the rate of degradation will decline. The results and resolution of this research can be a powerful component for further investigation and integrated planning of the study area.

Acknowledgements

Firstly, I would like to express my sincere gratitude to my supervisor Mr. Rony Basak, Assistant professor, Dept. of GEE, SUST for the constant support during this research and also for his patience, motivation, and profuse knowledge. I also wish to express my grateful thanks to Dr. Md. Sirajul Islam, Associate professor, Department of Geography and Environment, University of Dhaka, Md Mostafizur Rahman, Specialist, Database, ICT and System Management Division of CEGIS, A.B.M. Sarowar Alam and Animesh Ghosh from IUCN for their consistent support during my project pursuit. I take this opportunity to express gratitude to all the faculty members and stuffs of dept. of GEE, SUST for their kind help and sincere support.

References

- Ali, D.F., 2014. Wetland biodiversity a case study of Tanguar Haor by.
- Alphan, H., 2003. Land-use change and urbanization of Adana, Turkey. *Land Degrad. Develop.* 14 (6), 575–586.
- Bangladesh Centre for Advance Studies, 1997. Socio-economic Survey in Reed-land Forest Areas, vol. 1, Dhaka.
- BFD (Bangladesh Forest Department), 2012. Ecotourism in Bangladesh: Tanguar Haor. Ministry of Environment and Forest, Government of Bangladesh (accessed on 3 January 2012).
- Blasco, F., Aizpuru, M., 1997. Classification and evolution of the mangroves of India. *Trop. Ecol.* 38 (2), 357–374.
- Chander, G., Markham, B., 2003. Revised Landsat-5 TM radiometric calibration procedures and postcalibration dynamic ranges. *IEEE Trans. Geosci. Remote Sens.* 41 (11), 2674–2677.
- Chander, G., Markham, B.L., Helder, D.L., 2009. Summary of current radiometric calibration coefficients for Landsat MSS, TM, ETM+, and EO-1 ALI sensors. *Remote Sens. Environ.* 113 (5), 893–903.
- Houghton, R.A., 1994. The worldwide extent of land-use change. *Bioscience* 44 (5), 305–313.
- Islam, S.N., 2010. Threatened wetlands and ecologically sensitive ecosystems management in Bangladesh. *Front. Earth Sci. China* 4 (4), 438–448.
- Jensen, J.R., 2005. *Introductory Digital Image Processing: A Remote Sensing Perspective*. Pearson Prentice Hall, Upper Saddle River, NJ, USA.
- Lopez, A.D., Mathers, C.D., Ezzati, M., Jamison, D.T., Murray, C.J., 2006. Global and regional burden of disease and risk factors, 2001: systematic analysis of population health data. *Lancet* 367 (9524), 1747–1757.
- Markham, B.L., Barker, J.L., 1987. Thematic Mapper bandpass solar exoatmospheric irradiances. *Int. J. Remote Sens.* 8 (3), 517–523.
- Markham, B.L., Storey, J.C., Williams, D.L., Irons, J.R., 2004. Landsat sensor performance: history and current status. *IEEE Trans. Geosci. Remote Sens.* 42 (12), 2691–2694.
- Mayor-gordove, D., 2014. Information Sheet on Ramsar Wetlands (RIS) – 2009–2014 version, 7(2124), 12–22.
- McFeeters, S.K., 1996. The use of the Normalized Difference Water Index (NDWI) in the delineation of open water features. *Int. J. Remote Sens.* 17 (7), 1425–1432.
- Muttitanon, W., Tripathi, N.K., 2005. Land use/land cover changes in the coastal zone of Ban Don Bay, Thailand using Landsat 5 TM data. *Int. J. Remote Sens.* 26 (11), 2311–2323.
- Nackaerts, K., Vaesn, K., Muys, B., Coppin, P., 2005. Comparative performance of a modified change vector analysis in forest change detection. *Int. J. Remote Sens.* 26 (5), 839–852.
- NERP, 1993. Wetland Resources Specialist Studies. Northeast Regional Water Management Project/FAP6. Canadian International Development Agency, Dhaka, Bangladesh.
- Ozesmi, S.L., Bauer, M.E., 2002. Satellite remote sensing of wetlands. *Wetlands Ecol. Manage.* 10 (5), 381–402.
- Reid, R.S., Kruska, R.L., Muthui, N., Taye, A., Wotton, S., Wilson, C.J., Mulatu, W., 2000. Land-use and land-cover dynamics in response to changes in climatic, biological and socio-political forces: the case of southwestern Ethiopia. *Landscape Ecol.* 15 (4), 339–355.
- Richards, J.A., 1995. *Remote Sensing Digital Image Analysis: An Introduction*. Springer-Verlag, 265–290.
- Scott, D.A. (ed.), 1989. A directory of Asian wetlands. IUCN, International Union for Conservation of Nature, Gland, Switzerland.
- Sobhan, I., Alam, A.B.M.S., Chowdhury, M.S.M., 2012. Biodiversity of Tanguar Haor: A Ramsar Site of Bangladesh, Volume II: Flora. IUCN Bangladesh Country Office, Dhaka, Bangladesh, pp. xii+236.
- Thuillier, G., Floyd, L., Woods, T.N., Cebula, R., Hilsenrath, E., Hersé, M., Labs, D., 2003. Solar irradiance reference spectra. Solar variability and its effects on climate, 171–194.
- Wilkie, D.S., Finn, J.T., 1996. *Remote Sensing Imagery for Natural Resources Monitoring: A Guide for First-Time Users*. Columbia University Press.